DOI: 10.1002/ejoc.200900479

Stable-Ion NMR Spectroscopy and GIAO-DFT Study of Carbocations Derived from Multibridged [3$_n$]Cyclophanes

Kenneth K. Laali,*[a][‡] Takao Okazaki,[b] Toshikazu Kitagawa,[b] and Teruo Shinmyozu[c]

Keywords: Cyclophanes / Protonation / Carbocations / Donor–accepter systems / Superacidic systems

Mono- and diprotonation of the tri-, tetra-, and pentabridged cyclophanes [3$_3$](1,3,5)cyclophane (**4**), [3$_4$](1,2,3,5)cyclophane (**5**), and [3$_5$](1,2,3,4,5)cyclophane (**6**) were realized, and NMR spectroscopic studies of the resulting carbocations are reported. Unlike [2.2]paracyclophane and its fluorinated analogs that are protonated at a position *ipso* to the ethano-bridge, the monocations derived from **4**, **5**, and **6** are protonated at the unsubstituted ring positions. Protonation regioselectivity in the dications is *pseudo-meta* for **4** and **5** at unsubstituted ring positions, but for more-crowded **6** the second protonation occurs at a position that is *ipso* to the trimethylene bridge. Transannular π–π interactions in the monocations are manifested in the observed proton deshielding in the unprotonated π-deck. DFT and GIAO-DFT were employed to study the mono- and dications for comparison with the solution studies in superacids. GIAO-derived ΔNICS(1)$_{zz}$ data for the [3$_n$]cyclophane monocations imply decreased aromaticity in the cofacial unprotonated arene, consistent with transannular donor–acceptor interactions.

Introduction

Synthesis, structural/conformational features, and chemical transformations of cyclophanes, in particular their electrophilic substitution chemistry and directive effects, have fascinated organic chemists for decades. Recent progress in cyclophane chemistry has been summarized in several authoritative chapters and books.[1]

It is almost four decades since Hefelfinger and Cram[2] reported the direct NMR spectroscopic observation of *ipso* monoprotonated [2.2]paracyclophane **1**H$^+$ in FSO_3H/SO_2ClF (Figure 1). A decade later, Hopf and associates[3] succeeded in the generation of the doubly *ipso* protonated **1**H$_2^{2+}$ in "magic acid"/SO_2ClF at –110 °C. Double *ipso* protonation in **1**H$_2^{2+}$ increases angle deformation, which in turn decreases charge–charge repulsion.

Two decades ago, we reported[4] the generation and NMR spectroscopic studies of stable monocations of tetrafluoro[2.2]paracyclophane (**2**) and octafluoro[2.2]cyclophane (**3**) by *ipso*-protonation in superacid media (**2**H$^+$ and **3**H$^+$, respectively; Figure 2).

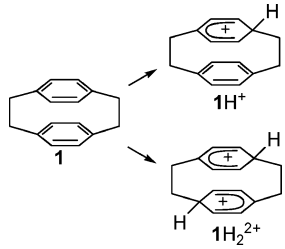

Figure 1. Mono- and diprotonation of parent **1**.

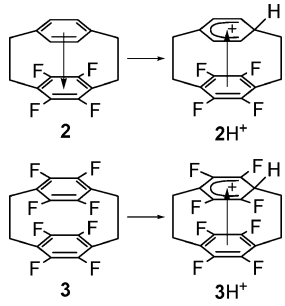

Figure 2. Stable arenium ions of fluorinated cyclophanes **2** and **3**.

Protonation of **2** leads to shielding of the arenium ion protons by the fluorinated deck, showing that the direction of transannular π-electron drain can be reversed upon the **2** → **2**H$^+$ transformation.

[a] Department of Chemistry, Kent State University, Kent, OH 44242, USA
[b] Department of Chemistry for Materials, Graduate School of Engineering, Mie University, Tsu 514-8507, Japan
[c] Institute of Materials Chemistry and Engineering, Graduate School of Sciences, Kyushu University, Hakozaki 6-10-1, Fukuoka 812-8581, Japan
[‡] Present address: Department of Chemistry, University of North Florida
Jacksonville, Florida 32224, USA
Fax: +1-904-620-3535
E-mail: kenneth.laali@UNF.edu

Supporting information for this article is available on the WWW under http://dx.doi.org/10.1002/ejoc.200900479.

In continuation of our studies on cyclophane cations[4–8] and annulenium ions[9–13] we report here on stable-ion NMR spectroscopy and computational studies of novel mono- and dications from tri-, tetra-, and pentabridged cyclophanes [3_3](1,3,5)cyclophane (**4**), [3_4](1,2,3,5)cyclophane (**5**), and [3_5](1,2,3,4,5)cyclophane (**6**; Figure 3).

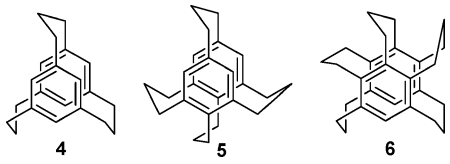

Figure 3. The tri-, tetra-, and pentabridged [3]cyclophanes. Each structure represents the most-stable conformer (**4b**, **5c**, or **6b**) by DFT calculations (see below).

Results and Discussion

Background to the Study

Synthesis of [3_3](1,3,5)cyclophane (**4**) was reported by Hübert[14a] and later by Misumi.[14b] Conformational studies of **4** (by VT-NMR) by Shinmyozu et al.[15] showed it to exist as two conformers with C_{3h} and C_s symmetry (with the latter being 0.4 kcal mol^{-1} more stable), and the energy barrier for the inversion of the trimethylene bridge is 12.4 kcal mol^{-1}. Shinmyozu et al.[16,17] devised an acid-catalyzed cyclization approach involving the *pseudo*-geminally substituted acetyl and chloromethyl groups to sequentially synthesize [3_4](1,2,3,5)cyclophane (**5**) and [3_5](1,2,3,4,5)-cyclophane (**6**; Figure 4). On the basis of their electronic spectra, transannular π–π interactions in the multibridged cyclophanes become more pronounced as the number of connecting trimethylene bridges increases.[16]

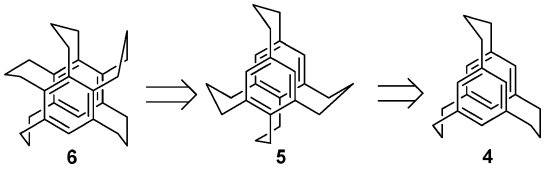

Figure 4. Sequential synthetic approach.

The conformational dynamics of **5** involving flipping of the trimethylene bridge were also studied by Shinmyozu et al.[18] by VT-NMR and MM3. The flipping of the trimethylene bridge was fast on the NMR timescale at room temperature, but became slower at low temperature, resulting in significant line broadening.[15–18]

NMR Spectroscopy and Computational Studies of Parent Cyclophanes 4–6

Structure optimization on triply bridged cyclophane **4** produced two minima with C_{3h} (**4a**) and C_s (**4b**) symmetries; the latter conformation is slightly more stable (see Table S1 in the Supporting Information). With cyclophane **5**, four minima were located, and **5c** was found to be the most stable. Finally, with pentabridged cyclophane **6**, three minima were located, and there was a clear preference for structure **6b**.

Since in earlier studies of the parent cyclophanes[15–18] the ^{13}C NMR spectroscopic data had not been specifically assigned, in the present study we employed 2D NMR techniques to assign all signals. The data are gathered in Figure S1. For comparison, the ^{13}C and ^{1}H NMR shifts were also computed by GIAO-DFT (see Figure S2). It can be seen that the computed values at the B3LYP/6-311+G(d,p)//B3LYP/6-31G(d) level are typically more deshielded than the solution data (see also later discussion).[19–21]

Persistent Monocations

Low-temperature reaction of cyclophanes **4**–**6** with FSO_3H/SO_2ClF at –70 °C resulted in the formation of monoprotonated cations **4**H$^+$, **5**H$^+$, and **6**H$^+$ (Figure 5). These cyclophanes were protonated at unsubstituted ring carbon atoms. The ^{1}H and ^{13}C NMR spectroscopic data for the monocations are gathered in Figure 6. Although the ^{13}C NMR spectrum of **5**H$^+$ was somewhat noisy, partial assignments could be made with the help of HMQC measurements. Resonances for protonated carbocations **4**H$^+$, **5**H$^+$, and **6**H$^+$ were broadened, owing to conformational dynamics involving flipping of the trimethylene bridges. Changing the temperature to between –90 and –50 °C afforded little improvement, and at –30 °C decomposition began to set in.

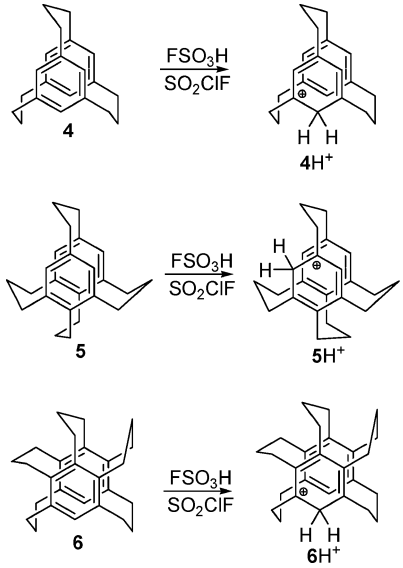

Figure 5. Protonation of [3_3](1,3,5)cyclophane (**4**), [3_4](1,2,3,5)-cyclophane (**5**), and [3_5](1,2,3,4,5)cyclophane (**6**) in FSO_3H/SO_2ClF. Each structure shows the most-stable conformation by DFT calculations (see later discussion).

The change in protonation regioselectivity in [3_n]cyclophanes as compared to [2.2]paracyclophane carbocations[2–5] (see also Figures 1 and 2) reflects diminished

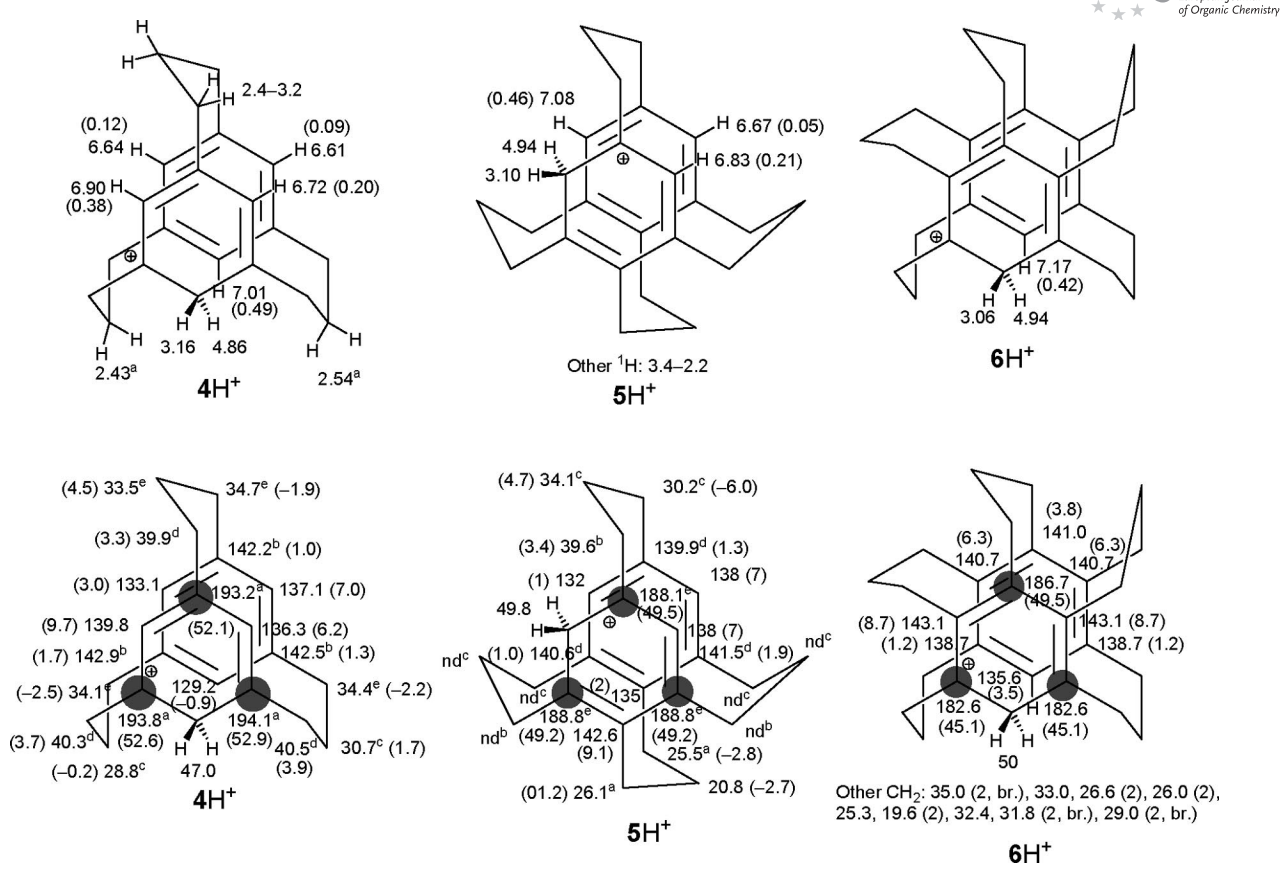

Figure 6. Summary of ^{1}H (above) and ^{13}C (below) NMR spectroscopic data for the monoprotonated cations derived from **4**–**6** in FSO_3H/SO_2ClF at –70 °C [a, b, c, d, and e (superscripts) denote interchangeable assignments for a pair or a group of resonances; change in δ^1H and δ^{13}C relative to those of the corresponding hydrocarbons in parentheses; dark circles signify the carbon atoms with high $\Delta\delta^{13}$C values].

charge–charge repulsion in the [3$_n$]cyclophanes, no longer requiring *ipso*-protonation/angle deformation at the bridge as a way to decrease charge–charge repulsion.

A notable feature in the ^{1}H NMR spectra of the carbocations is the diastereotopic nature of the CH_2 protons appearing at distinctly different environments. With the help of NOE it was established that the more-deshielded methylene proton is the one closest to the proton in the opposite deck. As depicted in Figure 7, transannular donor–acceptor effects and the loss of ring current in the [3$_n$]cyclophane carbocations are manifested in notable proton deshielding in the opposite deck.

For a comparison of relative protonation energies, structures located as minima, corresponding to various conformations, in tri-, tetra-, and pentabridged cyclophanes (Table S1) were protonated, and the resulting carbocations were computed by DFT. This showed that for each class of [3$_n$]cyclophanes, the carbocations derived from conformations with lower energy were generally more favored.

In accord with their arenium ion character, positive charge is strongly localized in the *ortho*/*para* positions relative to the protonation site, with near-equal $\Delta\delta^{13}$C values (cation minus neutral) for these positions in each case. Close inspection of the ^{13}C NMR spectroscopic data also reveals carbon deshielding at the ring carbon atoms of the opposite deck, consistent with transannular donor–acceptor interactions, although proton chemical shifts provide a more sensitive gauge of this effect.

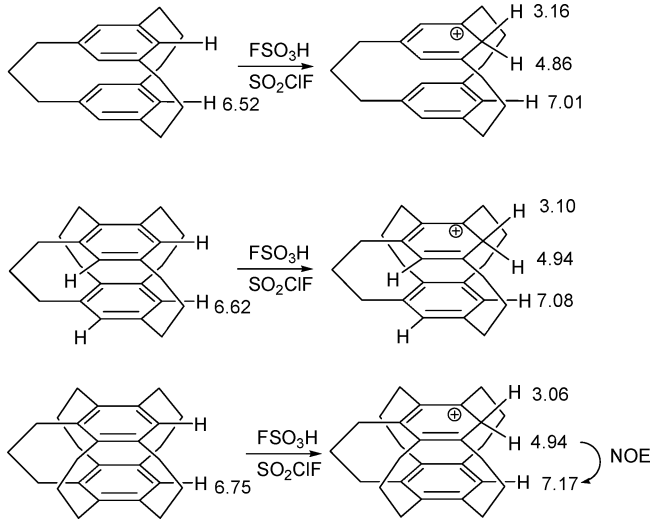

Figure 7. Transannular proton deshielding in the benzenium deck in protonated [3$_n$]cyclophanes.

The DFT-GIAO computed ^{13}C and ^{1}H chemical shifts for the monocations are summarized in Figure S3. As observed previously in various classes of other carbocations,[19–21] the ^{13}C shifts are more deshielded than the experimental solution NMR spectroscopic data [on average by about 10 ppm at the B3LYP/6-311+G(d,p) level], but the overall charge delocalization pattern is the same. The GIAO proton shifts are also more deshielded; nevertheless the GIAO-derived $\Delta\delta^{1}H$ values (cation minus neutral) are in concert with the solution data, clearly showing the operation of donor–acceptor interactions, which leads to notable proton deshielding in the opposite deck (Figures S2–S3).

The GIAO derived-NICS(1)$_{zz}$ data[20–25] (Figure 8) demonstrate that both cofacial decks in the neutral [3$_n$]cyclophanes are strongly aromatic. The more-negative NICS(1)$_{zz}$ values (increased aromaticity) on the inner (cofacial) decks reflect an extended π system spread over both cofacial rings. Increased aromaticity can be seen in polycyclic compounds with cofacial benzene rings generally.[25–28] Upon monoprotonation, the opposite deck becomes less aromatic, in accord with favorable donor–acceptor interactions in the cyclophane carbocation. On the basis of NICS(1)$_{zz}$, the outer face of the benzenium deck is no longer aromatic, whereas the inner face is still aromatic. This is likely due to interannular π–π interactions in the monocations.

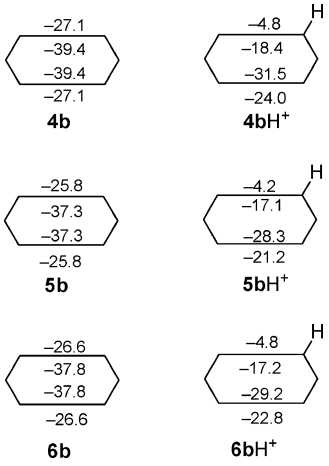

Figure 8. GIAO derived-NICS(1)$_{zz}$ data for the [3$_n$]cyclophanes and their protonated carbocations by B3LYP/6-311+(d,p)//B3LYP/6-31G(d) level.

Persistent Dications

Low-temperature reaction of [3$_n$]cyclophanes **4**–**6** with FSO_3H/SbF_5 (1:1)/SO_2ClF at –93 °C resulted in the formation of persistent diprotonated dications **4**H_2^{2+}, **5**H_2^{2+}, and **6**H_2^{2+} (Figure 9). A notable visual difference in the superacid solutions of the monocations and dications was the color of the solutions, which were red for the monocations (dark green in the case of **6**H^+) and yellow, yellow/orange, and yellow/brown for the dications (**4**H_2^{2+}, **5**H_2^{2+}, and **6**H_2^{2+} respectively). The color for the monocations could be attributed to charge transfer from the benzene rings to cationic decks owing to small energy gaps between HOMO and LUMO.[3] Tri- and tetrabridged cyclophanes **4** and **5** were protonated at the unsubstituted positions, but with the more sterically crowded [3$_5$](1,2,3,4,5)cyclophane (**6**), the second protonation occurred *ipso* to the trimethylene bridge to avoid severe repulsion between the two CH_2 groups resulting from diprotonation at two CHs. The NMR spectroscopic data were recorded at –93 °C. At this temperature, conformational flipping of the trimethylene bridges became too slow on the NMR timescale, resulting in extensive signal broadening. For most-crowded **6**H_2^{2+} this effect was so severe that only partial ^{1}H and ^{13}C NMR assignment could be made with the help of HMQC measurements. Attempts to induce conformational averaging and signal sharpening by raising the temperature to –70 °C led to gradual decomposition. The ^{1}H and ^{13}C NMR spectroscopic data for the dications are gathered in Figure 10.

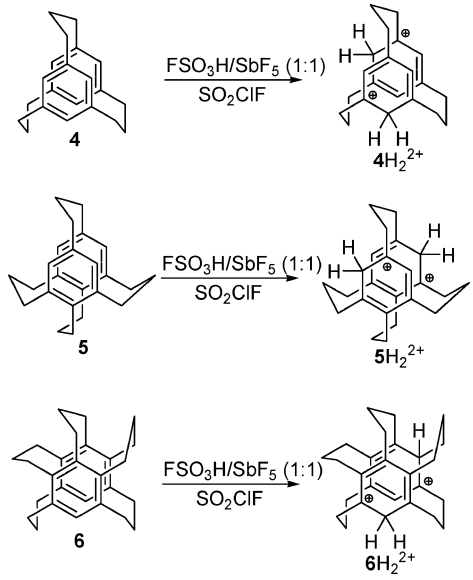

Figure 9. Diprotonation of [3$_3$](1,3,5)cyclophane (**4**), [3$_4$](1,2,3,5)-cyclophane (**5**), and [3$_5$](1,2,3,4,5)cyclophane (**6**) in FSO_3H/SbF_5 (1:1)/SO_2ClF at –90 °C.

The site of the second protonation for **6** could not be determined definitively by experimental NMR spectroscopy. Because only one aromatic CH proton was observed at δ = 7.84 ppm, the second protonation must have occurred *ipso* to the trimethylene bridge. Moreover, considering the preference for *pseudo-meta* diprotonation in cyclophanes **4** and **5**, it is likely that the structure is **6**H_2^{2+}, with the second protonation at a *pseudo-meta* position. This is supported by DFT calculations, which show that *pseudo-meta* diprotonation leads to the most stable dication (Table S1).

The ring CH_2s in dications **4**H_2^{2+} and **5**H_2^{2+} give rise to two pairs of diastereotopic resonances, whose assignments were secured by NOE. Judging from the $\Delta\delta^{13}C$ values, the magnitude of charge localization at the corresponding *ortho*/*para* positions is significantly larger in the dications than in the monocations.

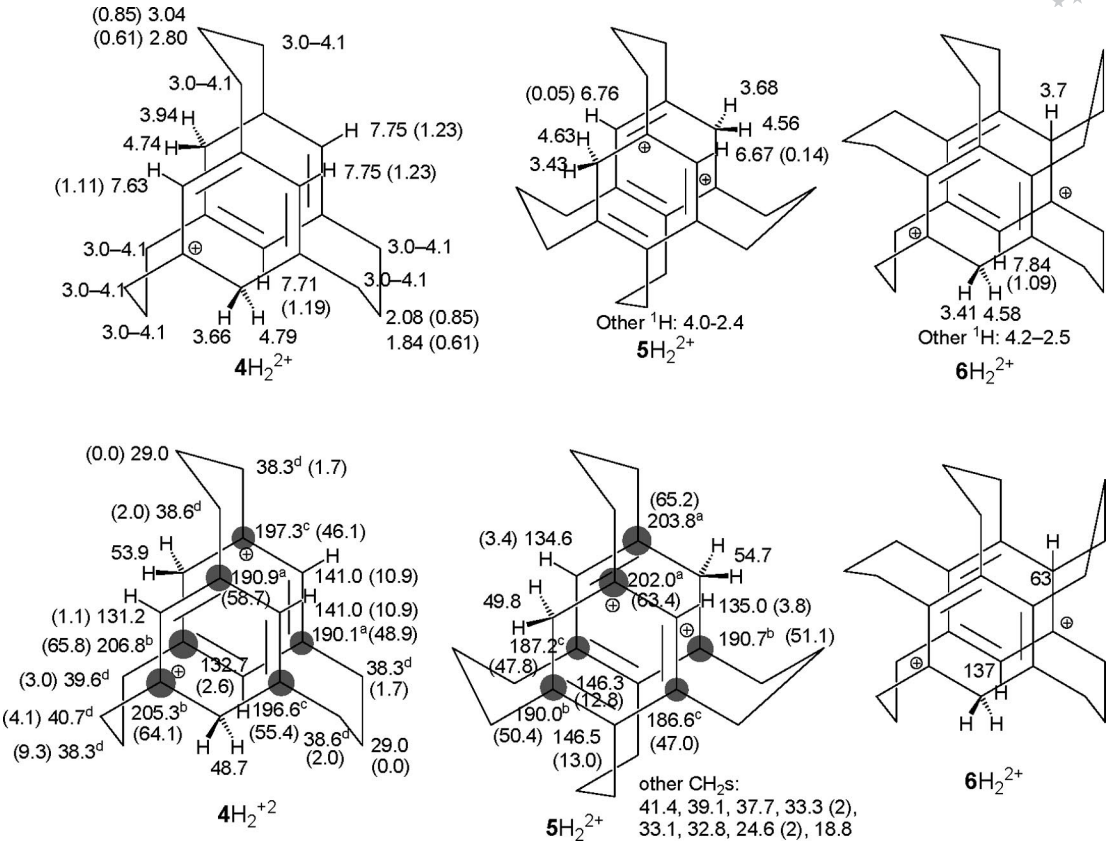

Figure 10. Summary of ^{1}H (above) and ^{13}C (below) NMR spectroscopic data for diprotonated cations derived from **4**, **5**, and **6** in FSO_3H/SbF_5 (1:1)/SO_2ClF at –93 °C [a, b, c, d (superscripts) denote interchangeable assignments for a pair or a group of resonances; change of δ^1H and δ^{13}C relative to those of the corresponding hydrocarbons in parentheses; dark circles signify the carbons with high $\Delta\delta^{13}$C values]; proton chemical shifts were corrected for bulk solvent effect (see Experimental Section).

Structures for possible diprotonated dications from **4**, **5**, and **6** were optimized by the DFT method and their energies are summarized in Table S1. *Pseudo-meta* diprotonated dications from **4**–**6** were the most stable and lower in energy than other dications by 4–5 kcal mol^{-1}. Energy differences among conformational isomers are small enough for interconversion.

The GIAO ^{13}C and ^{1}H data were also computed for the dications (Figure S4). As was noted for the monocations, the computed ^{13}C NMR chemical shifts for the dications at the B3LYP/6-311+G(d,p) level are more deshielded relative to the superacid data, but the overall charge delocalization patterns are the same.

Comparative Summary

Unlike [2.2]paracyclophanes that are protonated at a position *ipso* to the ethano bridge, low-temperature protonation of tri-, tetra-, and pentabridged cyclophanes [3$_3$](1,3,5)cyclophane (**4**), [3$_4$](1,2,3,5)cyclophane (**5**), and [3$_5$](1,2,3,4,5)cyclophane (**6**) with FSO_3H/SO_2ClF at –70 °C resulted in persistent monocations by protonation at the unsubstituted ring positions. This reflects diminished charge–charge repulsion in the [3$_n$]cyclophanes as compared to [2.2]paracyclophane, no longer requiring *ipso*-protonation/angle deformation as a way to decrease charge–charge repulsion. Charge delocalization mode in the resulting monocations is consistent with their arenium ion character. Transannular donor–acceptor interactions are manifested in deshielding of the opposite deck as determined by NMR spectroscopy and its diminished aromaticity as gauged by NICS(1)$_{zz}$. Low-temperature reaction of [3$_n$]cyclophanes **4**, **5**, and **6** with FSO_3H/SbF_5 (1:1)/SO_2ClF at –90 °C resulted in the formation of persistent diprotonated dications. Protonation regioselectivity in dications **4**H$_2^{2+}$ and **5**H$_2^{2+}$ was *pseudo-meta* at unsubstituted ring positions, but for more-crowded **6**H$_2^{2+}$, the second protonation occurred *ipso* to the trimethylene bridge. Charge delocalization in the cyclophane dications is consistent with the formation of two arenium ion decks with very high $\Delta\delta^{13}$C values for the *ortho*/*para* carbon atoms. A notable feature in the ^{1}H NMR spectra of both mono and dications is the diastereotopic nature of the CH_2 protons, appearing at distinctly different environments.

Experimental Section

General: ^{1}H NMR, ^{13}C NMR, and 2D NMR spectra were recorded with a 400 MHz NMR instrument. SO_2ClF was prepared according to a modified procedure of Prakash et al.[29] [3$_3$](1,3,5)Cyclo-

phane, [3$_4$](1,2,3,5)cyclophane, and [3$_5$](1,2,3,4,5)cyclophane were available from previous studies by Shinmyozu et al.[15–18] Their specific ^{1}H and ^{13}C NMR assignments are summarized in Figure S1 (Supporting Information). FSO_3H, FSO_3H/SbF_5 (1:1), and other reagents were commercially available and were used without purification.

Stable-Ion Generation Procedure: The substrate (5–8 mg) was placed in a 5-mm NMR tube and cooled to dry ice–ethanol temperature. SO_2ClF (ca. 0.5 mL) was condensed directly into the NMR tube and cold CD_2Cl_2 (2–3 drops) was introduced into the solution. Then, a few drops of FSO_3H were carefully introduced to prevent local overheating, whereupon an immediate color change took place. The NMR sample was vigorously stirred at the low temperature to give a homogeneous solution, which was analyzed by NMR experiments (^{1}H, ^{13}C, H/H COSY, HMQC, HMBC, and NOED).

The dications were prepared by protonation with FSO_3H/SbF_5 (1:1) at liquid N_2/ethanol bath, using an external sealed capillary tube containing [D$_6$]acetone instead of CD_2Cl_2. The reported ^{1}H NMR shifts in Figure S4 were corrected for bulk solvent effect according to Edlund et al.,[30] by adding 0.96 ppm to the ^{1}H shift values. Proton spectra gathered in the Supporting Information are the actual, uncorrected spectra.

The FSO_3H/SO_2ClF and FSO_3H/SbF_5 (1:1)/SO_2ClF solutions had the following colors: clear red and yellow for [3$_3$](1,3,5)cyclophane (**4**), red and yellow-orange for [3$_4$](1,2,3,5)cyclophane (**5**), and dark green and yellow-brown for [3$_5$](1,2,3,4,5)cyclophane (**6**), respectively.

Quenching Experiments: The cold superacid solutions were poured into a cold mixture of ice and sodium hydrogen carbonate and extracted with CH_2Cl_2. NMR spectroscopic analysis of the crude samples showed the recovery of the structurally intact cyclophane for **4**, a mixture of the intact cyclophane (20%) and several unknown compounds (80%) for **5**, and several unknown compounds for **6**. The identity of the newly formed compounds could not be determined due to extremely small quantities of the materials.

Computational Protocols: Structures were optimized using tight convergence from initial structures with a C_1 molecular point group by the density functional theory (DFT) method at the B3LYP/6-31G(d) level using the Gaussian 03 package.[31,32] All computed geometries were verified by frequency calculations to have no imaginary frequencies. Energies and molecular symmetry for the optimized structures are summarized in Table S1. NMR chemical shifts were calculated by the GIAO[33] (gauge-independent atomic orbital)-DFT method[34,35] at the B3LYP/6-311+G(d,p)//B3LYP/6-31G(d) level. NMR chemical shifts were referenced to TMS (GIAO magnetic shielding tensors were 31.98 ppm for ^{1}H and 184.1 ppm for ^{13}C in TMS; these values are related to the GIAO isotropic magnetic susceptibility), calculated with molecular symmetry of T_d or C_{3v} at the B3LYP/6-311+(d,p) level of theory. Nucleus independent chemical shifts (NICS)[36] were calculated at 1 Å above the ring center, denoted as NICS(1),[37] by the GIAO method at the B3LYP/6-311+G(d,p)//B3LYP/6-31G(d) level. The ring centers were defined as the simple average of Cartesian coordinates for all the carbon atoms in the ring. Planes of the rings were calculated by least-square methods using coordinates of all the carbon atoms in the ring. The "out-of-plane" components of the NICS tensors were calculated at 1 Å above the ring centers by rotating the planes of the rings orthogonal to the z axis, which is denoted as NICS(1)$_{zz}$.[38]

Supporting Information (see also the footnote on the first page of this article): DFT-calculated energies; Cartesian coordinates for the optimized structures; specific NMR assignments for the cyclophanes; GIAO-derived NMR spectroscopic data; selected NMR spectra for the carbocations.

[1] Recent review: R. Gleiter, R. Roers in *Modern Cyclophane Chemistry* (Eds.: R. Gleiter, H. Hopf), Wiley-VCH, Weinheim, **2004**, ch. 4; H. Hopf in *Modern Cyclophane Chemistry* (Eds.: R. Gleiter, H. Hopf), Wiley-VCH, Weinheim, **2004**, ch. 7; W. Sander in *Modern Cyclophane Chemistry* (Eds.: R. Gleiter, H. Hopf), Wiley-VCH, Weinheim, **2004**, ch. 8; H. Hopf, *Classics in Hydrocarbon Chemistry*, Wiley-VCH, Weinheim, **2000**, ch. 12.
[2] D. T. Hefelfinger, D. J. Cram, *J. Am. Chem. Soc.* **1971**, *93*, 4754–4767.
[3] H. Hopf, J.-H. Shin, H. Volz, *Angew. Chem. Int. Ed. Engl.* **1987**, *26*, 564–565.
[4] K. Laali, R. Filler, *J. Fluorine Chem.* **1989**, *43*, 415–427.
[5] K. K. Laali, E. Gelerinter, R. Filler, *J. Fluorine Chem.* **1991**, *53*, 107–126.
[6] K. K. Laali, D. A. Forsyth, *J. Org. Chem.* **1993**, *58*, 4673–4680.
[7] K. K. Laali, J. J. Houser, R. Filler, Z. Kong, *J. Phys. Org. Chem.* **1994**, *7*, 105–115.
[8] K. K. Laali, T. Okazaki, R. H. Mitchell, *J. Chem. Soc. Perkin Trans. 2* **2001**, 745–748.
[9] T. Okazaki, K. K. Laali, *Org. Biomol. Chem.* **2006**, *4*, 3085–3095.
[10] K. K. Laali, S. Bolvig, T. J. Raeker, R. H. Mitchell, *J. Chem. Soc. Perkin Trans. 2* **1996**, 2635–2638.
[11] K. K. Laali, M. Tanaka, R. H. Mitchell, D. Y. K. Lau, *J. Org. Chem.* **1998**, *63*, 3059–3066.
[12] K. K. Laali, T. Okazaki, R. H. Mitchell, T. R. Ward, *J. Org. Chem.* **2001**, *66*, 5329–5332.
[13] K. K. Laali, T. Okazaki, R. H. Mitchell, K. Ayub, R. Zhang, S. G. Robinson, *J. Org. Chem.* **2008**, *73*, 457–466.
[14] a) A. J. Hubert, *J. Chem. Soc. C* **1967**, 6–10; b) T. Otsubo, M. Kitasawa, S. Misumi, *Bull. Chem. Soc. Jpn.* **1979**, *52*, 1515–1520.
[15] T. Meno, K. Sako, M. Suenaga, M. Mouri, T. Shinmyozu, T. Inazu, H. Takemura, *Can. J. Chem.* **1990**, *68*, 440–445.
[16] T. Shinmyozu, S. Kusumoto, S. Nomura, H. Kawase, T. Inazu, *Chem. Ber.* **1993**, *126*, 1815–1818.
[17] T. Shinmyozu, M. Hirakida, S. Kusumoto, M. Tomonou, T. Inazu, J. M. Rudzinzki, *Chem. Lett.* **1994**, 669–672.
[18] Y. Sakamoto, N. Miyoshi, M. Hirakida, S. Kusumoto, H. Kawase, J. M. Rudzinski, T. Shinmyozu, *J. Am. Chem. Soc.* **1996**, *118*, 12267–12275.
[19] K. K. Laali, T. Okazaki, F. Sultana, S. D. Bunge, B. K. Banik, C. Swartz, *Eur. J. Org. Chem.* **2008**, 1740–1752.
[20] T. Okazaki, J.-H. Chun, K. K. Laali, *ARKIVOC* **2009**, 51–67.
[21] K. K. Laali, T. Okazaki, S. D. Bunge, D. Lenoir, *J. Org. Chem.* **2008**, *73*, 4092–4100.
[22] A. M. Piekarski, N. S. Mills, A. Yousef, *J. Am. Chem. Soc.* **2008**, *130*, 14883–14890; N. S. Mills, K. B. Llagostera, *J. Org. Chem.* **2007**, *72*, 9163–9169.
[23] Z. Chen, T. Heine, P. v. R. Schleyer, D. Sundholm in *Calculation of NMR and EPR Parameter: Theory and Applications* (Eds.: M. Kaupp, M. Bühl, V. G. Malkin), Wiley-VCH, Weinheim, **2004**, ch. 24, pp. 395–407.
[24] H. Fallah-Bagher-Shaidaei, C. S. Wannere, C. Corminboeuf, R. Puchta, P. v. R. Schleyer, *Org. Lett.* **2006**, *8*, 863–866.
[25] T. Okazaki, K. K. Laali, *Org. Biomol. Chem.* **2006**, *4*, 3085–3095.
[26] N. Mireles, R. Salcedo, L. E. Sansores, A. Martínez, *Int. J. Quantum Chem.* **2000**, *80*, 258–263.
[27] G. F. Caramori, S. E. Galembeck, *J. Phys. Chem. A* **2008**, *112*, 11784–11800.
[28] C. Corminboeuf, P. v. R. Schleyer, P. Warner, *Org. Lett.* **2007**, *9*, 3263–3266.
[29] V. P. Reddy, D. R. Bellew, G. K. S. Prakash, *J. Fluorine Chem.* **1992**, *56*, 195–197.

[30] B. Eliasson, D. Johnels, I. Sethson, U. Edlund, *J. Chem. Soc. Perkin Trans. 2* **1990**, 897–900.
[31] W. Koch, M. C. Holthausen, *A Chemist's Guide to Density Functional Theory*, 2nd ed., Wiley-VCH, Weinheim, **2000**.
[32] M. J. Frisch, G. W. Trucks, H. B. Schlegel, G. E. Scuseria, M. A. Robb, J. R. Cheeseman, J. A. Montgomery Jr, T. Vreven, K. N. Kudin, J. C. Burant, J. M. Millam, S. S. Iyengar, J. Tomasi, V. Barone, B. Mennucci, M. Cossi, G. Scalmani, N. Rega, G. A. Petersson, H. Nakatsuji, M. Hada, M. Ehara, K. Toyota, R. Fukuda, J. Hasegawa, M. Ishida, T. Nakajima, Y. Honda, O. Kitao, H. Nakai, M. Klene, X. Li, J. E. Knox, H. P. Hratchian, J. B. Cross, C. Adamo, J. Jaramillo, R. Gomperts, R. E. Stratmann, O. Yazyev, A. J. Austin, R. Cammi, C. Pomelli, J. W. Ochterski, P. Y. Ayala, K. Morokuma, G. A. Voth, P. Salvador, J. J. Dannenberg, V. G. Zakrzewski, S. Dapprich, A. D. Daniels, M. C. Strain, O. Farkas, D. K. Malick, A. D. Rabuck, K. Raghavachari, J. B. Foresman, J. V. Ortiz, Q. Cui, A. G. Baboul, S. Clifford, J. Cioslowski, B. B. Stefanov, G. Liu, A. Liashenko, P. Piskorz, I. Komaromi, R. L. Martin, D. J. Fox, T. Keith, M. A. Al-Laham, C. Y. Peng, A. Nanayakkara, M. Challacombe, P. M. W. Gill, B. Johnson, W. Chen, M. W. Wong, C. Gonzalez, J. A. Pople, *Gaussian 03*, Revision B.05, Gaussian, Inc., Pittsburgh, PA, **2003**.
[33] K. Wolinski, J. F. Hinton, P. Pulay, *J. Am. Chem. Soc.* **1990**, *112*, 8251–8260; R. Ditchfield, *Mol. Phys.* **1974**, *27*, 789–807.
[34] G. Schreckenbach, T. Ziegler, *J. Phys. Chem.* **1995**, *99*, 606–611.
[35] H.-U. Siehl, V. Vrček in *Calculation of NMR and EPR Parameter. Theory and Applications* (Eds.: M. Kaupp, M. Bühl, V. G. Malkin), Wiley-VCH, Weinheim, **2004**, ch. 23, pp. 371–394.
[36] P. v. R. Schleyer, C. Maerker, A. Dransfeld, H. Jiao, N. J. R. van Eikema Hommes, *J. Am. Chem. Soc.* **1996**, *118*, 6317–6318.
[37] P. v. R. Schleyer, M. Manoharan, Z.-X. Wang, B. Kiran, H. Jiao, R. Puchta, N. J. R. van Eikema Hommes, *Org. Lett.* **2001**, *3*, 2465–2468.
[38] C. Corminboeuf, T. Heine, G. Seifert, P. v. R. Schleyer, J. Weber, *Phys. Chem. Chem. Phys.* **2004**, *6*, 273–276.

Received: May 4, 2009
Published Online: July 31, 2009

